World Academy of Science, Engineering and Technology
International Journal of Chemical and Molecular Engineering
Vol:6, No:8, 2012

Porous Ni and Ni-Co Electrodeposits for Alkaline Water Electrolysis – Energy Saving

I. Herraiz-Cardona, C. González-Buch, E. Ortega, V. Pérez-Herranz, J. García-Antón

***Abstract*—**Hydrogen is considered to be the most promising candidate as a future energy carrier. One of the most used technologies for the electrolytic hydrogen production is alkaline water electrolysis. However, due to the high energy requirements, the cost of hydrogen produced in such a way is high. In continuous search to improve this process using advanced electrocatalytic materials for the hydrogen evolution reaction (HER), Ni type Raney and macro-porous Ni-Co electrodes were prepared on AISI 304 stainless steel substrates by electrodeposition. The developed electrodes were characterized by SEM and confocal laser scanning microscopy. HER on these electrodes was evaluated in 30 wt.% KOH solution by means of hydrogen discharge curves and galvanostatic tests. Results show that the developed electrodes present a most efficient behaviour for HER when comparing with the smooth Ni cathode. It has been reported a reduction in the energy consumption of the electrolysis cell of about 25% by using the developed coatings as cathodes.

***Keywords*—**Alkaline water electrolysis, energy efficiency, porous nickel electrodes

I. Introduction

HYDROGEN is considered an ideal energy carrier that can be an alternative to fossil fuels. It is a clean, versatile and efficient fuel [1]-[3]. Exceptional energy per mass content, storage and transportation possibilities, safety features, and reduced harmful emissions are few advantages of this substance as an energy carrier [4]. The electrochemical production of hydrogen by alkaline water electrolysis is one of the most promising methods with great potential of using renewable energy sources, such us solar energy. Also it represents an environmentally friendly technology. Nevertheless, the high production costs due to low conversion efficiency and electrical power expenses can be named as the main drawbacks of electrochemical hydrogen production [4], [5]. In order to make this technique more efficient and competitive, both the decrease of the overpotentials of electrode reactions and the selection of inexpensive electrode materials with good electrocatalytic activity are needed. The electrode activity can be enlarged by increasing the real surface area and/or the intrinsic activity of the electrode material [6].

All the authors are with the Ingeniería Electroquímica y Corrosión (IEC) group, Departamento de Ingeniería Química y Nuclear, Universitat Politècnica de València, Camino de Vera s/n, 46022 Valencia, Spain. (phone: +34-96-387-76-32; fax: +34-96-387-76-39; e-mail: jgarciaa@iqn.upv.es)

This work was supported by Generalitat Valenciana (Project PROMETEO/2010/023) and Universitat Politècnica de València ((PAID-06-10-2227)

For this purpose, the most important and most studied electrode material is nickel, its alloys and compounds, because of its stability and favourable activity [7]-[10]. One of the common ways to enlarge the real surface area is the utilization of Raney-type alloys from which the active component (Al, Zn) is dissolved by alkaline leaching. Caustic leaching of the alloy is accompanied by volume losses leading to pore and crack formation, yielding a highly porous catalytic nickel surface suitable for use in alkaline water electrolysis [11]-[14]. These materials are characterized by small pore diameters, which cause a strong variation of the concentration of the dissolved molecular hydrogen inside the pore during the HER. The consequence of this concentration gradient is that only a small fraction of the interfacial surface is efficiently used. On this context, macro-porous nickel electrodes can be of great interest as an alternative to Raney-Nickel since, although they have smaller roughness factors, their electrodic surface is much more accessible. One technique used to fabricate macro-porous electrodes is the galvanic deposition at very high current densities [15].

On the other hand, the intrinsic activity of Ni has been enlarged by alloying Ni with some metals: NiCo; NiLa; NiMo; NiW; NiFe; etc. [6]. It has been demonstrated that alloying Ni with Co, in a composition range between 41 and 64 weight percent, can improve the intrinsic catalytic activity as a consequence of the synergism among the catalytic properties of nickel (low hydrogen over-potential) and of cobalt (high hydrogen adsorption) [16].

The aim of the present work is the development of a Ni/Zn Raney type electrode and a macroporous Ni-Co electrode in order to evaluate their suitability for the most economical electrolysis process. The activity towards hydrogen evolution of these electrodes was assessed by recording hydrogen discharge curves, and series of galvanostatic tests, simulating the conditions in the normal operation of an alkaline electrolyser.

II. Experimental

A. Preparation of Electrodes

The metallic coatings were deposited on an AISI 304 stainless steel cylindrical substrate, embedded in Teflon, leaving a cross-sectional available area of 0.5 cm^2. AISI 304 stainless steel as substrate material was mainly chosen due to its good mechanical and corrosion resistance at relatively low cost.

Before the electrodeposition experiments, the stainless steel substrate was mechanically polished with emery paper down to 4000 grit, next it was degreased for 1 min with 25 wt.% NaOH at 90 ºC, immersed in HCl 18 wt.% during 1 min, and anodically treated in 70 wt.% H_2SO_4 at 108 mA/cm^2 for 3 min. Then the substrate surface was struck at -27 mA/cm^2 in a Wood's nickel solution (240 g/L $NiCl_2$, 120 mL/L HCl) for 5 min, in order to produce a thin, adherent deposit of nickel which serves as a base for the subsequent electrodeposition. Between each treatment the electrode was rinsed with distilled water. Nickel type Raney alloy depositions (NiR electrodes) were performed galvanostatically at a current density of -50 mA/cm^2, from a modified Watts Bath in which NaCl was substituted by $NiCl_2$. After the electrodeposition, the electrodes were treated in 6 M NaOH solution at 50 ºC during 48 hours. Treatment in alkali dissolves a percentage of the electrodeposited zinc, producing a porous nickel layer of high surface area [12], [13].

In order to obtain a macro-porous superficial morphology, a nickel-cobalt electrode was constructed galvanostatically at a very high current density (1000 mA/cm^2) in a bath initially composed of $NiCl_2{\cdot}6(H_2O)$ and NH_4Cl (NiHcd electrode). After 45 min, an amount of $CoCl_2{\cdot}6(H_2O)$ was added to the electrodeposition process, which was prolonged up to 60 min maintaining the operating conditions, in order to avoid the Co occlusion down to a Ni layer, as a consequence of the anomalous co-deposition of Ni-Co alloys, where Co is preferentially deposited [17].

TABLE I
BATH COMPOSITIONS AND EXPERIMENTAL CONDITIONS USED IN THE ELECTRODEPOSITION OF ELECTROCATALYTIC COATINGS

Electrode	Bath Composition (g/L)		Experimental Conditions	
NiR	$NiSO_4{\cdot}6(H_2O)$	330	Temperature (ºC)	50
	$NiCl_2{\cdot}6(H_2O)$	45	j_d (mA/cm^2)	50
	H_3BO_3	37	Time (min)	60
	$ZnCl_2$	20	pH	4.5
NiHcd	$NiCl_2{\cdot}6(H_2O)$	48	Temperature (ºC)	25
	$CoCl_2{\cdot}6(H_2O)$	10	j_d (mA/cm^2)	1000
	NH_4Cl	170	Time (min)	60
			pH	4.5

Since the hydrogen overvoltage of the substrate is low to generate hydrogen gas in highly acidic media and at high cathodic current densities, a large number of hydrogen bubbles created on the substrate move towards the electrolyte/air interface during the Ni electrodeposition process. Thus, the metal growth towards the gas bubble is prohibited simply because there are no metal ions available there, leading the electrodeposition between the gas bubbles, following the schema shown in Fig. 1. In other words, the hydrogen bubbles function as a dynamic template during metallic deposition.

Table I summarizes the bath compositions and the experimental conditions used to the synthesis of the electrodes. The reagents used for electrolyte preparation were of chemical grade and were no subjected to an additional purification. Distilled water was used to prepare electrolytes.

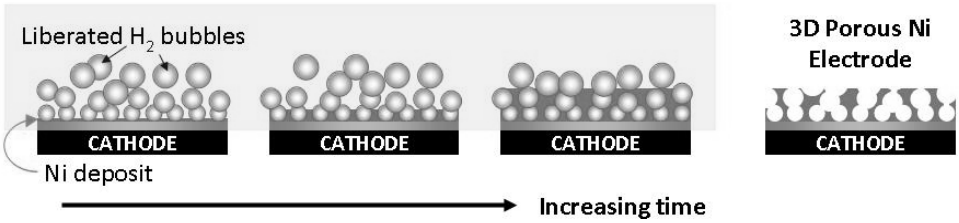

Fig. 1 Simplified description of the formation process of the NiHcd electrodes

Electrodepositions were carried out in a thermostated one-compartment cell made of Pyrex glass with a Teflon cover having adequate holes to lodge the electrodes and entrances to add reagents to the bath. The solution inside the cell had an initial volume of 50 mL, and the substrate surface was placed in horizontal position, allowing the free release of the produced hydrogen bubbles. The counter electrode was a large-area platinum electrode of high purity. The reference electrode was a commercially available silver-silver chloride (Ag-AgCl) electrode with 3 M potassium chloride (KCl) solution. The experiments were accomplished by using an Autolab PGSTAT302N potentiostat/galvanostat. The structures, morphologies and compositions of the developed electrodes were examined by means of a JEOL JSM-3600 scanning electron microscope coupled with an Energy-Dispersive X-Ray (EDX) Spectrometer, and an OLIMPUS LEXT OLS3100-USS confocal laser scanning microscope.

B. Electrochemical Measurements

The developed electrodes were characterized by means of hydrogen discharge curves and galvanostatic tests.

In order to obtain the hydrogen discharge curves, a progressively increasing voltage was applied, starting from 0 V between the anode (smooth Ni) and cathode (working electrode) and going up to - 3 V. With the aid of these curves, the minimum discharge potentials were experimentally determined for each electrode pair.

The galvanostatic experiments were carried out at three different applied current densities of 20, 50 and 100 mA/cm^2 and at six different temperatures: 30, 40, 50, 60, 70 and 80 ºC, during 1 hour. The electrochemical measurements were carried out in an electrochemical cell developed by the Dpto. Ingeniería Química y Nuclear of the Polytechnic University of Valencia [18].

It is a three-electrode cell that allows monitoring the volume of gas generated at the anode and the cathode. Also, this system has a heating circuit to control the temperature.

III. Results and Discussion

A. Morphology and Chemical Composition of NiR and NiHcd Electrodes

The confocal laser scanning 3D micrographs shown in Fig.2 illustrate the extend morphology of the electrodeposits obtained according to the experimental conditions reported in Table I. As it is clear from Fig. 2, the superficial morphology of both electrodes consists of a continuous matrix with cavities and pores distributed in the whole surface.

Whereas the NiR electrode (Fig.2.a) is characterized by a cracked surface, the macro-porosity of the NiHcd electrode is provided by quasy-cylindrical pores (Fig.2.b.), developed according to the electrodeposition strategy discussed in the experimental section. The electrodes also differ in the superficial composition determined by EDX. On the one hand, the NiR layer, after the leaching treatment, contains about 59.6 wt.% of nickel, and 40.4 wt.% of zinc. Therefore, after the leaching treatment, there is still a high percentage of zinc present in the coatings, which corresponds to the zinc occluded down to a Ni layer. On the other hand, the NiHcd layer is composed of 56.3 wt.% of nickel and 43.7 wt.% of cobalt.

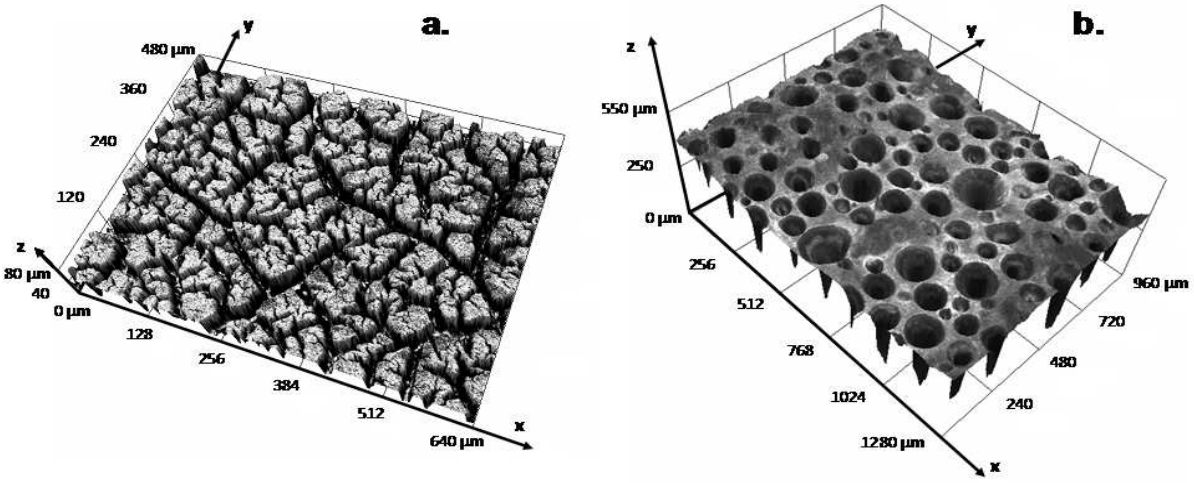

Fig. 2 Three-dimensional micrographs of the developed electrodes obtained by means of the confocal laser-scanning microscope OLYMPUS LEXT OLS3100-USS: a. NiR; b. NiHcd

B. Electrochemical Characterization

In order to evaluate the suitability of the developed cathode for the most economical electrolysis process, both current-cell potential curves (hydrogen discharge curves) and galvanostatic tests have been carried out. All these tests where performed in the P200803389 cell [18].

Fig. 3 shows the hydrogen discharge curves obtained in 30 wt.% KOH solution at different temperatures using the developed electrodes as cathodes. The curves performed on commercial smooth Ni electrode were also included to compare the obtained results. As seen in Fig.3, after the discharge of gasses, there is a rapid increase in the current with increasing applied voltage, because of the evolution of hydrogen at the cathode and oxygen at the anode. The discharge of gasses starts at lower potential for the NiR electrode, and the current passing through the solution is larger with this cathode, compared with both the NiHcd and the smooth Ni cathode, at all potentials. Nevertheless, at 80ºC the behavior of the NiHcd electrode considerably improves, and the evolution of gasses starts practically at the same potential value than that reported for the NiR cathode.

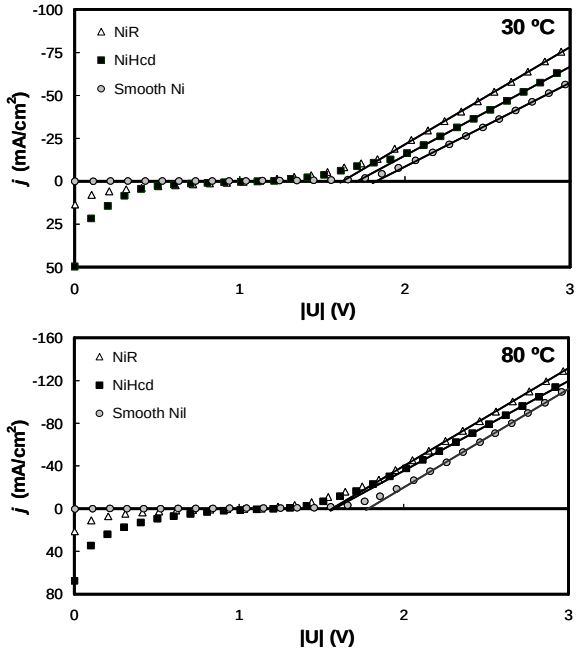

Fig. 3 Hydrogen discharge curves obtained in KOH 30 wt.% at different temperatures

The minimum hydrogen discharge potentials (E_{H2}), given in

Table II, were experimentally determined by extrapolating the linear part of the hydrogen discharge curves (between 2 and 3 V) to the zero current, as described elsewhere [19].

As it is shown in Table II, the E_{H2} values decrease with temperature due to the increased conductivity of the electrolyte and higher electrode activities. The reversible discharge potential for water splitting (E_{rev}) also reduces with an increase in operating temperature as given by the relation [20], [21]:

$$E_{rev}(T/K)=1.5184-1.5421\cdot10^{-3}\cdot T+9.523\cdot10^{-5}\cdot T\cdot lnT+9.84\cdot10^{-8}\cdot T^{2} \quad (1)$$

The difference between the measured and theoretical calculated values of these systems (E_{H2}-E_{rev}) can be taken to be the experimental overpotential, which represents the voltage in excess of the thermodynamic voltage required to overcome the losses in the cell (η_{H2}). As it is clear from the data in Table II, the developed electrodes manifest lower η_{H2} values than that registered for the smooth Ni electrode, being the NiR the best overall cathode. This reduction can be attributed to the lower cathodic overpotential associated with the reaction kinetics (electrode polarization effects) in the synthesized electrodes with respect to the smooth commercial Ni electrode, which is mainly attributed to a higher surface area. It is also seen in Table II that the higher the temperature the higher the catalytic activity of the NiHcd electrode, reaching an η_{H2} very close to that reported for the NiR electrocatalyst. It can be explained according to the chemical composition of the electrodes. Ni-Co alloys, in the composition range of the NiHcd electrode, manifest a synergism between the properties of nickel (high catalytic activity) and cobalt (high hydrogen adsorption), that can be emphasized at high temperatures, where the electrochemical hydrogen adsorption is worse realized [16].

TABLE II
HYDROGEN DISCHARGE POTENTIALS AND OVERPOTENTIALS

Parameter	Temperature (ºC)					
	30	40	50	60	70	80
Smooth Ni						
E_{H2} (V)	1.830	1.820	1.810	1.801	1.794	1.780
η_{H2} (V)	0.605	0.604	0.602	0.602	0.603	0.597
NiR						
E_{H2} (V)	1.620	1.600	1.581	1.570	1.560	1.551
η_{H2} (V)	0.395	0.384	0.373	0.370	0.369	0.368
NiHcd						
E_{H2} (V)	1.711	1.701	1.686	1.665	1.630	1.574
η_{H2} (V)	0.486	0.485	0.478	0.466	0.439	0.383

Galvanostatic tests have been carried out in order to verify the performance behavior of these alloys in long duration experiences for the HER, at different current densities and temperatures.

Fig. 4a reports the cell voltage for a temperature of 50ºC at different current densities for the NiR catalyst. Notwithstanding the small potential oscillation, the registered cell voltage (between anode and cathode) can be considered to be rather stable. It can be appreciated an increase in the cell voltage with the current density. The inverse effect in the cell voltage is obtained when the temperature is increased for a same current density (50 mA/cm^2, in Fig. 4.b). On the other hand, as it is shown in the histograms of Fig. 4, the hydrogen production remains practically constant with the variation in temperature, increasing directly with the current density applied.

Fig. 5 shows the cell voltage obtained on the characterized electrodes at 20 mA/cm^2 and 40ºC. The lowest cell potential was registered for the NiR electrode, corroborating the results obtained from the hydrogen discharge curves study. It is important to point out that it has not been recorded loses in the catalytic activity, unexpected increases in the cell potential for a same current density applied, during the application of the set of galvanostatic tests, consolidating the stability of the developed deposits.

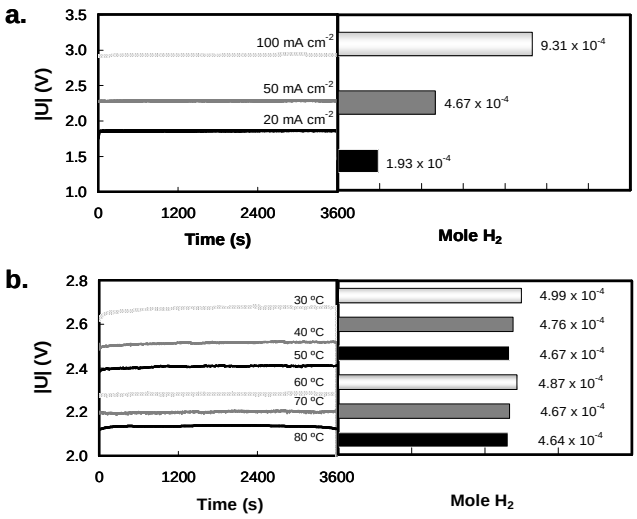

Fig. 4a Effect of applied current density on the cell voltage and the hydrogen production at 50ºC; and b. Effect of temperature on the cell voltage and the hydrogen production at 50 mA/cm^2, for the NiR electrode

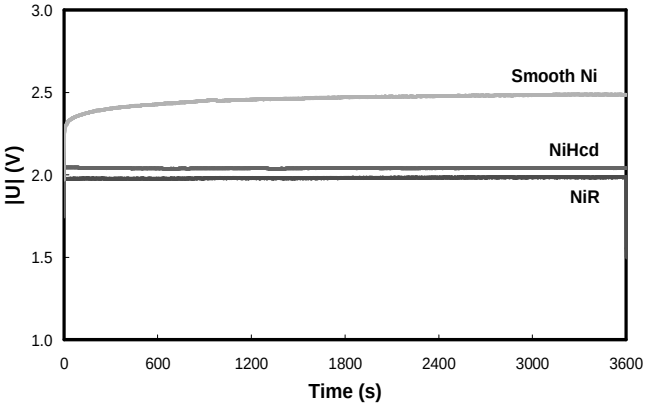

Fig. 5 Cell voltage obtained on the characterized electrodes in KOH 30 wt.% at 20 mA/cm^2 and 40ºC

The energy requirements for the electrolytic hydrogen

evolution process are calculated using the relation:

$$Q_{H2} = \frac{I \cdot U \cdot t}{mole\ H_2} \quad (2)$$

where Q is the energy consumption per one mole of hydrogen evolved (kJ/mole), I is the absolute applied current in A, U is the cell voltage in V and t is the time in s. To obtain the correct number of hydrogen moles, the hydrogen pressure was determined as follows:

$$P_{H_2} = P_{atm} + \rho(T)gh - P_v(T) \quad (3)$$

where P_{atm} is the atmospheric pressure, $\rho(T)$ is the mass density of a 30 wt. % KOH solution, g is the gravitational acceleration, h is the height difference between the liquid levels of the cathodic and central compartments, and $P_v(T)$ is the water saturation pressure in 30 wt.% KOH solutions. In this way, the moles of evaporated water at the temperature conditions can be subtracted from the measured volume in the cathodic compartment of the voltammeter. The determined energy consumptions for all the characterized electrodes are presented in Fig. 6. It is shown an expected type of dependence: increase of the energy consumption with the increase of current density. Moreover, the energy requirement decreases with increasing temperature. In principal, that means the higher the temperature the higher the reaction rate, thus the lower voltage requested for a certain current density. As it is clearly shown in Fig. 6, energy consumption of the electrolysis cell decreases for about 25% using the developed catalyst coatings as cathodes in the conditions at which it is produced the industrial alkaline water electrolysis, i.e. at the highest current densities and 80ºC, with respect to the commercial smooth Ni electrode.

C. Energy efficiency

When temperature is considered, it is accurate to use the higher heating value voltage (E_{HHV}) for efficiency calculation [20]. E_{HHV} corresponds to the heat content of the dry product gases with respect to the liquid water at 25 ºC. Therefore,

$$\varepsilon = \frac{E_{HHV}}{U} \quad (4)$$

where ε is the energy efficiency.

The absolute temperature dependence of E_{HHV} can be given by the relation [21], [22]:

$$E_{HHV}(T/K) = 1.4146 + 2.205 \cdot 10^{-4} \cdot T + 1.0 \cdot 10^{-8} \cdot T^2 \quad (5)$$

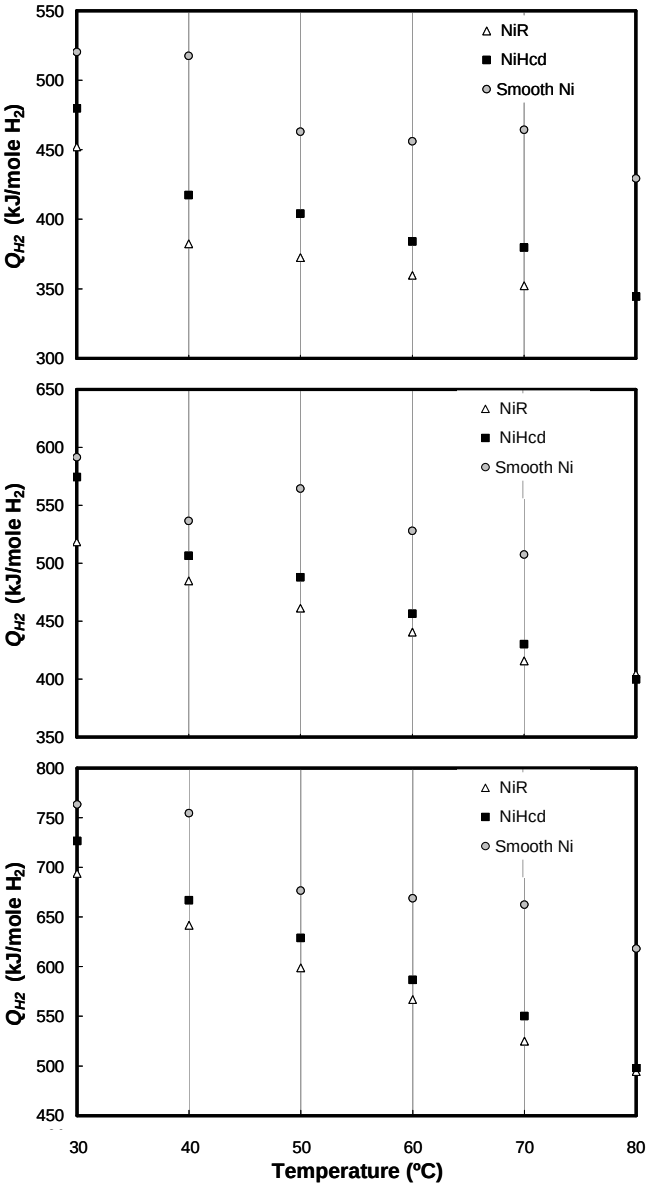

Fig. 6 Energy consumption of the electrolysis cell for the characterized electrodes in KOH 30 wt.% at different current densities and temperatures

E_{HHV} increases slightly with temperature, taking a value of 1.494 V at 80 ºC. In order to determine the maximum efficiency of the hydrogen evolution process, the minimum hydrogen discharge potentials, E_{H2} shown in Table II, can be used as the cell voltage (U) in (4). As it is shown in Table III, higher energy efficiencies for a hydrogen production are obtained at higher operating temperature conditions, because of an increase in the mobility of the molecules and ions. Moreover, the higher energy efficiencies are obtained for the NiR electrode, although the behavior of both developed electrodes is very close at the highest temperature.

The energy efficiency, ε, was also determined for each point of the Q_{H2} values plotted in Fig.6, obtaining the 3D diagram of Fig. 7.

As it is shown, the efficiency of the electrolysis is inversely proportional to the cell potential [2]. Therefore, as the cell potential increases with the electrolysis current, it can be seen that the efficiency slightly decreases at increasing H_2 production. The obtained efficiencies of the unity electrolysis cell can not be compared to that reported in literature, due to the specific cell geometry. Nevertheless, it has been observed an improvement in the energy efficiency of the developed electrodes of about 10-35 % when comparing with the commercial nickel electrode.

TABLE III
MAXIMUM ENERGY EFFICIENCIES

Electrode	Temperature (ºC)					
	30	40	50	60	70	80
Smooth Ni	0.81	0.82	0.82	0.83	0.83	0.84
NiR	0.92	0.93	0.94	0.95	0.96	0.96
NiHcd	0.87	0.87	0.88	0.89	0.92	0.95

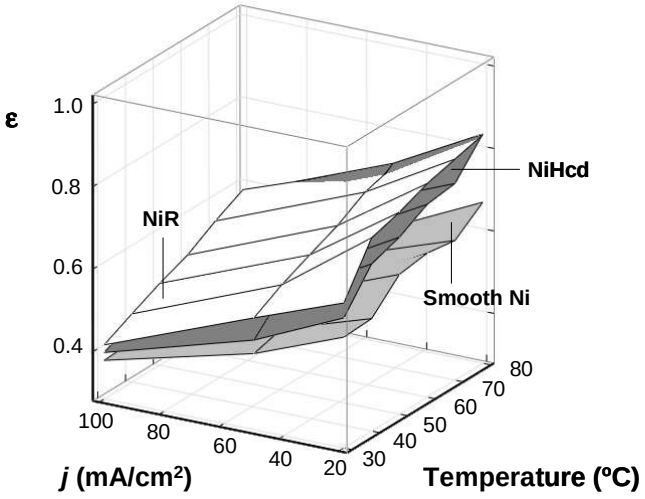

Fig. 7 3-D diagram of the efficiency of the electrolysis cell.Comparison between the smooth pure Ni and the developed electrodes

IV. CONCLUSION

Nickel type Raney layers (NiR) and Ni-Co deposits obtained at high current densities (NiHcd) were successfully developed by electrodeposition, and characterized morphologically and electrochemically for hydrogen evolution reaction (HER) in alkaline media, showing significant electrocatalytic effects. From both hydrogen discharge curves and galvanostatic tests it has been pointed out that energy savings per mass unit of electrochemically evolved hydrogen from aqueous solutions on the developed electrodes, can be beyond 25% in some cases, compared with the standard nickel electrodes, being the NiR electrode the best overall catalyst. Nevertheless, at 80ºC (the usually employed temperature for the industrial process) the behavior of the NiHcd electrode is very close to that reported for the NiR layer.

This phenomenon can be explained according to the chemical composition of the NiHcd electrode. The presence of Co (43.7 wt.%) improves the intrinsic catalytic activity of the electrode, specially at high temperature, compensating the lower roughness factor of the macroporous surface, when comparing with the NiR cracked structure.

The electrocatalytic achievement and obtained stability of the developed electrodes appears valuable in the view of the significant energy savings, which is relevant for the possible use in industrial applications.

ACKNOWLEDGMENT

I. Herraiz-Cardona is grateful to the Ministerio de Ciencia e Innovación (Spain) for a postgraduate grant (Ref. AP2007-03737).

REFERENCES

[1] F. Barbir, "Transition to renewable energy systems with hydrogen as an energy carrier," Energy vol. 34, pp. 308–312, 2009.
[2] S.A. Sherif, F. Barbir, T.N. Veziroglu, "Wind energy and the hydrogen economy-review of the technology," Solar Energy, pp. 647–660, 2005.
[3] M.R. Rahimpour, A. Mirvakili, K. Paymooni, "Hydrogen as an energy carrier: A comparative study between decalin and ciclohexane in thermally coupled membrane reactors in gas-to-liquid technology," Int. J. of Hydrogen Energy, pp 6970-6984, 2011.
[4] K. Mazloomi, C. Gomes, "Hydrogen as an energy carrier: Prospects and challenges," Renewable and Sustainable Energy Reviews, pp. 3024-3033, 2012.
[5] J.C. Ganley, "High temperature and pressure alkaline electrolysis," Int. J. of hydrogen energy, pp. 3604-3611, 2009.
[6] Lasia A. Hydrogen Evolution. In: Vielstich W, Lamm A, Gasteiger HA, editors. Handbook of fuel cell technology, John Wiley and Sons Ltd; 2003, p. 416-440.
[7] K. Zeng , D. Zhang, "Recent progress in alkaline water electrolysis for hydrogen production and applications," Progress in Energy and Combustion Science, vol. 36, pp.307–326, 2010
[8] A.E. Mauera, D.W. Kirk, S.J. Thorpe, "The role of iron in the prevention of nickel electrode deactivation in alkaline electrolysis," Electrochimica Acta , vol. 52, pp. 3505–3509, 2007.
[9] R. Solmaz, A. Döner, I. Sxahinb, A.O. Yüce, G. Kardasx, B. Yazıcı, M. Erbil, "The stability of NiCoZn electrocatalyst for hydrogen evolution," Int. J. of hydrogen energy, vol. 34, pp. 7910-7918, 2009.
[10] M.P. Marceta Kaninski, S.M. Miulovic, G.S. Tasic, A.D. Maksic, V.M. Nikolic, "A study on the Co-W activated Ni electrodes for hydrogen production from alkaline water electrolysis – Energy saving," *Int. J. of hydrogen energy*, vol. 36, pp. 52274-5235, 2011.
[11] Y. Choquette, L. Brossard, A. Lasia, H. Menard., "Investigation of hydrogen evolution on Raney-Nickel composite-coated electrodes," Electrochim Acta vol 35, pp. 1251-1256, 1990.
[12] L. Chen, A. Lasia, "Study of the kinetics of hydrogen evolution reaction on Nickel-Zinc alloy electrodes". J Electrochem Soc, vol. 138, pp. 3321-3328, 1991.
[13] L. Birry, A. Lasia, "Studies of the hydrogen evolution reaction on Raney nickel-molybdenum electrodes", J Appl Electrochem, vol. 34, pp. 735-749, 2004.
[14] R. Solmaz, G. Kardas. "Hydrogen evolution and corrosion performance of NiZn coatings," Energy Conv. Manag., vol 48, pp. 583-591, 2007.
[15] C.A. Marozzi, A.C. Chialvo, "Development of electrode morphologies of interest in electrocatalysis. Part 2: Hydrogen evolution reaction on macroporous nickel electrodes," Electrochimica Acta, vol. 46, pp. 861–866, 2001.
[16] C. Lupi, A. Dell'Era, M. Pasquali, "Nickel-cobalt electrodeposited alloys for hydrogen evolution in alkaline media," Int. J. of hydrogen energy, vol. 34, pp. 2101-2106, 2009.
[17] A. Brenner, "Electrodeposition of alloys: Principles and practices," vol. 2, Academic Press Inc., New York, 1963.

[18] García-Antón J, Blasco-Tamarit E, García-García DM, Guiñón-Pina V, Leiva-García R, Pérez-Herranz V. 2008: P200803389.
[19] B. Yazici, G. Tatli, H. Galip, M. Erbil, "Investigation of suitable cathodes for the production of hydrogen gas by electrolysis," Int. J. Hydrogen Energy, vol. 20, pp. 957-965, 1995.
[20] RL. LeRoy, "Industrial water electrolysis: Present and future," Int. J. Hydrogen Energy, vol. 8, pp. 401-417, 1983.
[21] RL LeRoy, CT. Bowen, DJ. Leroy, "The thermodynamics of aqueous water electrolysis," J. Electrochemical Society, vol. 127, pp. 1954-1962, 1980.
[22] J. Divisek, "Water electrolysis in a low and medium temperature regime," in *Electrochemical production and combustion of hydrogen*, H. Wendt, Ed. Elsevier Publishing Company, 1990, pp.137-212.